Mechanism of CO_2 Hydration: Porous Metal Oxide Nanocapsule Catalyst Can Mimic the Biological Carbonic Anhydrase Role†

Nuno A. G. Bandeira,[a] Somenath Garai,[b] Achim Müller[b] and Carles Bo[a,c]

[a] *Dr. N. A. G. Bandeira, Prof. C. Bo*
Institute of Chemical Research of Catalonia (ICIQ). Avda. Països Catalans, 16. 43007 Tarragona (Spain).
E-mail: cbo@iciq.cat
[b] *S. Garai, Prof. A. Müller*
Fakultät für Chemie, Universität Bielefeld, Postfach 100131, 33501 Bielefeld (Germany).
[c] *Prof. C. Bo*
Department Química Física i Inorgànica. University Rovira i Virgili. Marcel·li Domingo s/n. 43007 Tarragona (Spain).

† Dedicated to the memory of Tom Ziegler (1945-2015).

Electronic Supplementary Information (ESI) available: See
DOI: 10.1039/x0xx00000x

The mechanism for the hydration of CO_2 within a Keplerate nanocapsule is presented. A network of hydrogen bonds across the water layers in the first metal coordination sphere facilitates the proton abstraction and nucleophilic addition of water. The highly acidic properties of the polyoxometalate cluster are crucial in explaining the catalysed hydration.

Concerns about global warming, together with the incoming necessity to find alternative feedstocks to fossil fuels,[1] have boosted interest in the capture and use of CO_2 as a chemical starting material.[2-5] Living organisms having the carbonic anhydrase enzyme carry out the simplest CO_2 transformation, i.e. hydration to
carbonic acid, in an easy manner. The presence of an electrophilic Zn center together with a network of water molecules in the proximity of the enzyme site makes the hydration reaction possible,
which is rather slow in the absence of catalyst. The exploration of carbonic anhydrase[6-9] and related analogues[10] has afforded major bio-

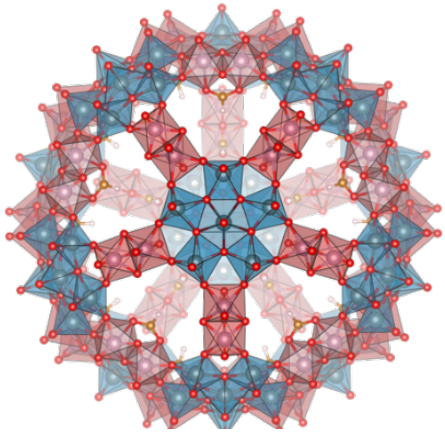

Figure 1. The pictorial representation of the $\{Mo_{132}\}$ Keplerate capsule.

inspired catalytic routes for CO_2 fixation over the past decades. On the other hand, synthetic chemistry afforded new transition metal based catalysts that can convert CO_2 into other chemical entities, for instance CO_2 reduction to methanol,[11] coupling with oxiranes to produce cyclic carbonates,[12-14] or other value added chemicals.[15, 16]
Some of us reported recently[17] a novel way for sequestrating and transforming CO_2 into carbonate by encapsulation within unique molybdenum oxide nanocapsules. These capsules, belonging to the Keplerate family, are nano-sized molecular metal oxide spheres with the general formula $[\{(M^{VI})M^{VI}{}_5O_{21}(H_2O)_6\}_{12}\{M'^{V}{}_2O_2X_2(\mu^2\text{-}Y)\}_{30}]^{n-}$ (M=Mo, W; M'=Mo; X=O, S; Y=bridging ligand, e.g. $RCOO^-$,SO_4^{2-}).[18] This sort of capsule contains 12 pentagonal $\{Mo^{VI}{}_6\}$ units placed at the vertices of an icosahedron and linked by 30 binuclear $\{Mo^{V}{}_2\}$ units. This arrangement leads to the formation of capsules (Figure 1) with twenty $\{M_3Mo_6O_9\}$-type pores and a cavity where a large quantity of water molecules, anions or other species can be confined.[19, 20] By bubbling CO_2 in a solution of $(NH_4)_{42}[\{(Mo^{VI})Mo^{VI}{}_5O_{21}(H_2O)_6\}_{12}\{Mo^{V}{}_2O_4(\mu^2\text{-}CH_3COO)\}_{30}]\cdot$ ca. 10 $CH_3COONH_4\cdot$ ca. 300 $H_2O \equiv (NH_4)_{42}\cdot$**Anion 1a**$\cdot$ ca. 10 $CH_3COONH_4\cdot$ ca. 300 $H_2O \equiv$ **Compound 1**[21] at pH 7 the carbonate derivative $(NH_4)_{72}$ $[\{(Mo^{VI})Mo^{VI}{}_5O_{21}(H_2O)_6\}_{12}\{Mo^{V}{}_2O_4(\mu^2\text{-}CO_3)\}_{30}]\cdot$ ca. 260 $H_2O \equiv (NH_4)_{72}\cdot$ **Anion 2a**$\cdot$ ca. 260 $H_2O \equiv$ **Compound 2** was obtained.[17] The ***Figure 2.*** The pictorial representation of the $\{Mo_{132}\}$ Keplerate outcome of these results urged the major question of whether the carbonate anion formed in solution (in minute amounts at pH 7) was captured by the Keplerate sphere, or more interestingly, whether the carbonate anion formation took place *in situ* inside the capsule, either at the Mo^{V} or Mo^{VI} coordination sites, by a metal catalysed nucleophilic addition of water to a solubilised CO_2 molecule, likewise the accepted mechanism of carbonic anhydrase.

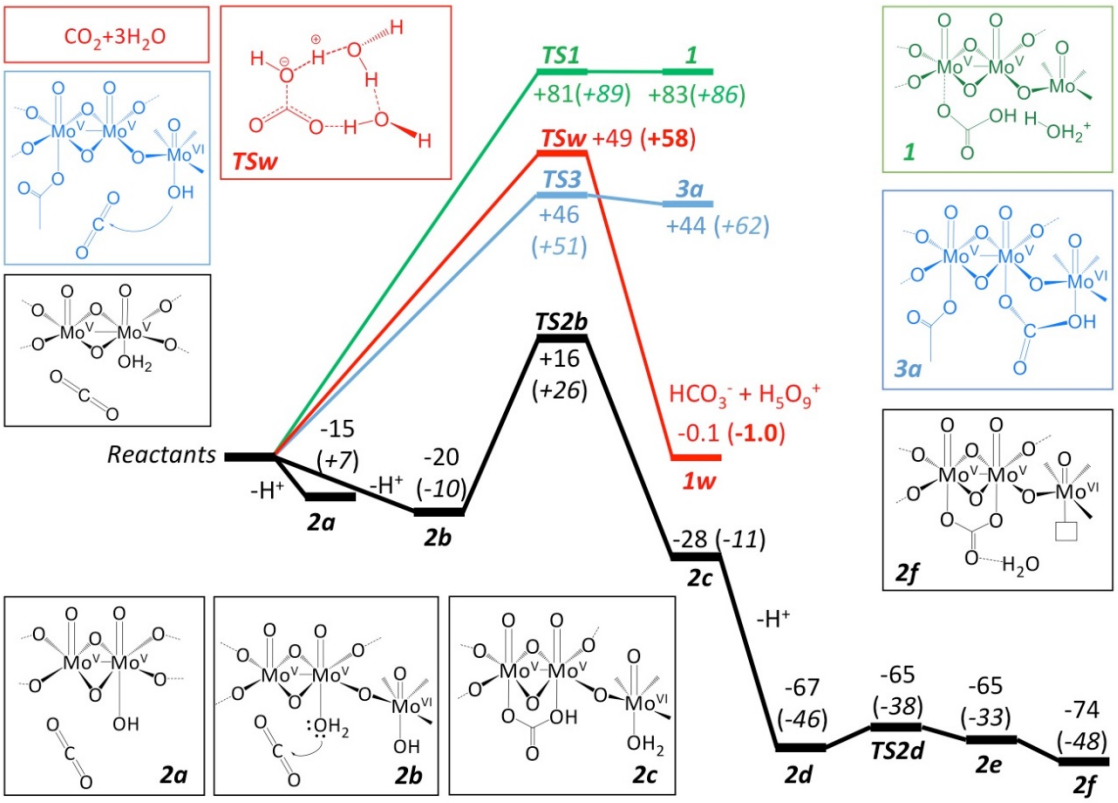

Figure 3. Several mechanistic pathways for CO_2 hydration. (red) Uncatalysed reaction; (green, blue, black) Catalysed reaction. Electronic energies and Gibbs free energies in parenthesis evaluated using a partial Hessian. All energies in $kJ.mol^{-1}$.

The CO_2 transformation is also reversible via acidification of the aqueous solution of **Compound 2**.[17] The results of the theoretical study presented herein suggest that this transformation of CO_2 to carbonate is actually the third example[22, 23] known to date of a catalytic process occurring inside the $\{Mo_{132}\}$ capsule, where the Mo^{V} and also the Mo^{VI} sites play a role.

The mechanism of the hydration of CO_2 to form the carbonic acid has been a subject of theoretical studies over the past decades.[24, 25] The challenge lies in the accurate description of the explicit water molecules participating in the reaction as was shown by the latest work of Yamabe and Kawagishi.[26] The uppermost energy barrier of carbon dioxide hydration is always the initial step of water addition.[27] The arrangement of this initial transition state[24-26, 28] is a cyclic three water molecular arrangement such as the one depicted in Figure 2. We will adopt this model as a benchmark to compare with our own calculations on the catalytic sequestration of CO_2 and its conversion into the carbonate form.

In a recent study we demonstrated that by using a cluster model of the $\{Mo_{132}\}$ nanocapsule, the reaction pathway of the reversible cleavage of methyl-tert-butyl ether[22] was successfully unravelled. The model assembly was defined to mimic the nature of the active sites of the Keplerate and it was formulated as $[\{(Mo^{VI})Mo^{VI}{}_5O_{13}(OH)_8\}_2\{Mo^{V}{}_2O_4\}]^{6+}$ containing two pentagonal $\{(Mo^{VI})Mo^{VI}{}_5\}$-units and one linker unit of the type $\{Mo^{V}{}_2O_4\}$. It fully retained the essential characteristics of the $\{Mo_{132}\}$ reactive sites and therefore we have selected that model for the present study. Since the formation of the carbonate anion takes place in aqueous media, the presence of water molecules inside the Keplerate sphere must play an essential role in the reaction and therefore it is essential that the cluster model should incorporate a sufficiently large number of water molecules. Thus we included 13 additional water molecules explicitly in this study, so the model used is formulated as $[\{(Mo^{VI})Mo^{VI}{}_5O_{13}(H_2O)_6(OH)_8\}_2\{Mo^{V}{}_2O_4(H_2O)\}]^{6+}$, which leaves one vacant coordination site for the interaction/coordination of CO_2 to one of the two Mo^{V} centres, while the second one bears a water molecule which is supposed to be highly reactive.

As expected the CO_2 molecule being nonpolar, does not coordinate to Mo^{V} centre either in η^1 or η^2 fashion. Notwithstanding, we could characterize a weakly bound stationary point structure in which CO_2 is hydrogen-bonded to the water molecule in one Mo^{V} centre and to a water molecule on Mo^{VI}, thus located in the vicinity of the reactive centre. This will be our starting point (named ***Reactants***) for the reaction path studies defining the zero of energies.

The highest energy reaction path explored ***TS1*** (Figure 2) is perhaps the most intuitive pathway involving a concerted nucleophilic addition of an aqua ligand to CO_2 followed by the subsequent proton rejection and formation of a local Zundel cation ($H_5O_2^+$) sponsored by the hydrogen bonding of the neighbouring aqua ligands. Note that the neighbouring water ligands coordinated to Mo^{VI} centres contribute to stabilizing the rejected proton and the concomitant formation of bicarbonate. Although we explored multiple conformational possibilities, a coordinated adduct of the type $\{O_2C\text{-}OH_2\}$ could not be obtained.

Owing to the accumulation of positive charge closer to the metal centres, ***TS1*** transition state is shown to be too excessively high in energy (+89 $kJ.mol^{-1}$) to become a competitive pathway vis-à-vis the unassisted ***TSw*** transition state for hydration of CO_2.

In light of these results we explored a different route that yielded a bicarbonate coordinated intermediate resulting from a nucleophilic addition of a hydroxo to CO_2. Given that the Mo^{VI} centres are more Lewis acidic than Mo^{V} the likely candidate for a good reactant would be ***2b*** bearing the {$Mo^{V}(OH_2)$-O-$Mo^{VI}(OH)$} unit rather than ***2a*** ({$Mo^{V}(OH)$-O-$Mo^{VI}(OH_2)$}). This is borne out by the relative energetics of the two isomers, which favour ***2b*** by some 5 kJ.mol^{-1}. The mechanism should expectedly involve a proton relay from the aqua-ligand in the Mo^{V} centre concerted with the nucleophilic addition of the hydroxo group to CO_2. The ΔG estimate for the ***2a***→***2b*** conversion is further widened to 17 kJ.mol^{-1} in favour of ***2b***.

The bicarbonate intermediate undergoes further deprotonation resulting in ***2d***. The release of a proton from ***2d*** through to ***2e*** has a negligible energy barrier (for ***TS2d***, 2 kJ. mol^{-1} in electronic or +8 kJ.mol^{-1} in free energy). The carbonate intermediate ***2e*** is approximately iso-energetic with its parent bicarbonate ***2d*** but can be easily converted to ***2f*** with lower free energy. The intermediate ***2f*** has one non-coordinated water molecule which stabilises the carbonate ligand via hydrogen bonding. The Mo-carbonate bond lengths in ***2e*** are 2.392 and 2.329 Å, which are within the error limits of the experimentally determined values.[12]

The higher acidity of the Mo^{VI} centre prompted us to explore another possible mechanistic route in which the direct nucleophilic addition

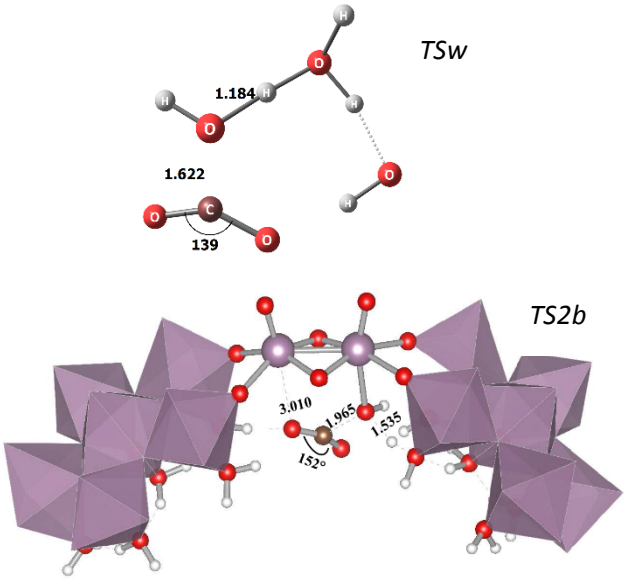

Figure 4. Transition state structures for the uncatalysed CO_2 + $3H_2O$ (TSw) and for the catalysed reaction (TS2b). Selected distances in Å and angles in degrees.

to the CO_2 molecule takes place directly by the hydroxo group coordinated to the Mo^{VI} sites while the vacant coordination site of Mo^{V} is utilized to stabilize the transition state. A subsequent backflip of bicarbonate or carbonate to the {Mo^{V}_2}-linker would be necessary to be consistent with the final carbonate adduct. The initial steps of this pathway are sketched in blue in Figure 2. The transition state ***TS3*** has a similar energy value to ***TSw*** (the uncatalysed transition state) but the intermediate ***3a*** is not sufficiently stable to be considered a viable route (see Supplementary material for these additional structures).

There are structural differences between the catalysed and uncatalysed systems namely with regards to each transition state which are summarised Figure 3. The Mayer-Mulliken bond orders[29] (MBO) were also analysed in the present case which reflect the bond strength between the different atoms in any given system. The most striking difference between ***TSw*** and ***TS2b*** is that the latter is a slightly "lesser bound" transition state with a reaction coordinate (C-O) bond order 0.377 whereas in ***TSw*** it is 0.557. The ∠(O-C-O) angles are also considerably different between ***TSw*** (139°) and ***TS2b*** (152°) consistent with a larger electron cloud of the incoming O(-C) and consequently a lower angular distortion of CO_2. The leaving proton is also more bound to the oxygen atom in ***TSw*** (MBO=0.430) than in ***TS2b*** (MBO=0.250). In the latter case the outgoing proton from the aqua ligand is already at a large distance (1.535 Å, see Figure 3).

Finally to predict the potential reactivity of related systems, additional calculations were carried out on model analogues of the {$W_{72}Mo_{60}$} and {W_{132}} nanocapsules. The former nanocapsule has been characterised[30] experimentally although the latter is still unknown. Since the key point in the mechanism is the generation of the nucleophilic hydroxo species coordinated to the star-shaped M^{VI} moieties, the relative thermodynamic stability of ***2a*** and ***2b*** species was determined. The calculated ΔE(***2a***→***2b***) is –65 kJ.mol^{-1} for the mixed W/Mo oxo-cluster model and –85 kJ.mol^{-1} for the hypothetical full W system. This points to a likely enhanced reactivity of the heavier metal Keplerates in the order {Mo_{132}}<{$W_{72}Mo_{60}$}<{W_{132}}. These results also indicate that W^{V} centres are less (Lewis) acidic with respect to W^{VI} than Mo^{V} in relation to Mo^{VI}.

Conclusions

DFT based calculations enabled unravelling the CO_2 hydration reaction pathway as evidenced involving **Compound 1** by considering the known mechanism in the aqueous solution. The *in situ* bicarbonate formation, promoted by the Mo^{V} centres, inside the capsule is excellent and less energetically demanding than direct carbonate uptake from aqueous solution. Three trials were performed in the present work, which can be summarised as follows:

i) A neutral charge pathway with an aqua ligand nucleophilic addition to CO_2 results in a high kinetic barrier $\Delta E^{\ddagger}$= +81 kJ/mol and a product of exceedingly high energy.

ii) A hydroxo ligand pathway in which the nucleophilic attack takes place on a Mo^{VI} site. This is an endergonic process requiring +46 kJ/mol to form a product.

iii) A hydroxo ligand pathway where the hydroxo group in an Mo^{VI} centre will act as a proton acceptor in tandem with the nucleophilic addition of CO_2 to an aqua ligand at the Mo^{V} sites. The activation energy $\Delta E^{\ddagger}$= +36 kJ/mol is the lowest of all the trials, even lower than the uncatalysed hydration reaction, and the ensuing product assembly is 28 kJ/mol more stable than the reactant assembly.

Therefore the most plausible mechanism for the formation of **Compound 2** will be the latter based on comparison of computed energies with respect to a comparable micro-solvated CO_2 hydration. The resemblance of the mechanism with that operating in the carbonic anhydrase enzyme is remarkable. The subtle differences lie in the first steps of the latter mechanism: the rate-limiting step is the protolysis of the aqua ligand in $(His)_3Zn\text{-}OH_2$[3b,4] which is then followed by a lower energy nucleophilic addition to CO_2 whereas the Keplerate acts in a concerted single step for both. These results pave the way for defining a new application of Keplerate anionic capsules as CO_2 storage nanodevices.

Computational Details

The Amsterdam Density Functional (ADF) program package[31] version 2012.01 has been used throughout. The Perdew, Burke and Ernzerhof (PBE)[32] gradient corrected exchange and correlation functionals were used in the calculations. The choice of this functional is due to the fairly accurate description it provides of hydrogen bonds,[33] an aspect which is crucial to this work. The ZORA[34, 35] scalar relativistic Hamiltonian was employed with a triple zeta Slater type orbital[36] (STO) augmented with one polarization function (TZP) for molybdenum, and double zeta STO type functions augmented with d functions on the remaining elements. A small frozen core was used for all the elements ($1s^2$ shell for O and C, and $3d^{10}$ shell for Mo) except hydrogen. The geometry optimizations were performed via the numerical integration scheme of Versluis and Ziegler.[37] Stationary points were located with a 5.0 digit integration accuracy whereas partial and full analytic hessian calculations were done with 7.0 digit integration accuracy. The COSMO[38] implicit solvation scheme was used throughout. The imaginary frequencies related to the reaction coordinate were followed by a small fraction of their coordinate displacement in either direction and subsequently re-optimized to achieve the reactant and product. Partial hessian calculations were performed on the reaction site, i.e. the eight atoms present in the ensemble $\{CO_2+OH_2+OH^-\}$ for ***2a***, ***2b***, ***TS2b***, and ***2c***. For the remainder of the steps seven atoms $\{HCO_3^-+OH^-\}$ were used to compute the partial hessian. Electronic and free energies of reactions leading to a formal loss of a proton were calculated via an explicit Brønsted type equilibrium between two water molecules and the Zundel cation ($H_5O_2^+$).

Notes and references

This work was funded by the Spanish Ministerio de Economia y Competitividad (MINECO) through project CTQ2014-52824-R, by the Generalitat de Catalunya project 2014SGR409, and by the ICIQ Foundation. The Severo Ochoa Excellence Accreditation (SEV-2013-0319) and the COST Action CM1203 "Polyoxometalate Chemistry for Molecular Nanoscience (PoCheMoN)" are gratefully acknowledged. NAGB gratefully acknowledges COFUND/Marie Curie action 291787-ICIQ-IPMP for funding. A.M. acknowledges continuous financial support by the Deutsche Forschungsgemeinschaft and the ERC (Brussels) for an Advanced Grant.

Keywords: CO2 activation • biological aspects • DFT mechanism • Keplerate • polyoxometalates.

1. M. Aresta, *Carbon Dioxide as Chemical Feedstock*, Wiley, 2010.
2. M. E. Boot-Handford, J. C. Abanades, E. J. Anthony, M. J. Blunt, S. Brandani, N. Mac Dowell, J. R. Fernández, M.-C. Ferrari, R. Gross, J. P. Hallett, R. S. Haszeldine, P. Heptonstall, A. Lyngfelt, Z. Makuch, E. Mangano, R. T. J. Porter, M. Pourkashanian, G. T. Rochelle, N. Shah, J. G. Yao and P. S. Fennell, *Energy Environ. Sci.*, 2014, **7**, 130-189.
3. J. J. Vericella, S. E. Baker, J. K. Stolaroff, E. B. Duoss, J. O. Hardin IV, J. Lewicki, E. Glogowski, W. C. Floyd, C. A. Valdez, W. L. Smith, J. H. Satcher Jr, W. L. Bourcier, C. M. Spadaccini, J. A. Lewis and R. D. Aines, *Nat. Commun.*, 2015, DOI: 10.1038/ncomms7124.
4. V. Bhola, F. Swalaha, R. Ranjith Kumar, M. Singh and F. Bux, *Int. J. Environ. Sci. Technol.*, 2014, **11**, 2103-2118.
5. A. Sanna, M. Uibu, G. Caramanna, R. Kuusik and M. M. Maroto-Valer, *Chem. Soc. Rev.*, 2014, **43**, 8049-8080.
6. K. D'Ambrosio, G. De Simone and C. T. Supuran, in *Carbonic Anhydrases as Biocatalysts*, eds. G. De Simone and C. T. Supuran, Elsevier, Amsterdam, 2015, ch. 2, pp. 17-30.
7. D. N. Silverman and R. McKenna, *Acc. Chem. Res.*, 2007, **40**, 669-675.
8. C. Greco, V. Fourmond, C. Baffert, P.-h. Wang, S. Dementin, P. Bertrand, M. Bruschi, J. Blumberger, L. de Gioia and C. Leger, *Energy Environ. Sci.*, 2014, **7**, 3543-3573.
9. J. K. J. Yong, G. W. Stevens, F. Caruso and S. E. Kentish, *J. Chem.Technol. Biotechnol.*, 2015, **90**, 3-10.
10. G. Parkin, *Chem. Rev.*, 2004, **104**, 699-768.
11. A. Goeppert, M. Czaun, J.-P. Jones, G. K. Surya Prakash and G. A. Olah, *Chem. Soc. Rev.*, 2014, **43**, 7995-8048.
12. K. R. Roshan, B. M. Kim, A. C. Kathalikkattil, J. Tharun, Y. S. Won and D. W. Park, *Chem. Commun.*, 2014, **50**, 13664-13667.

13. F. Castro-Gómez, G. Salassa, A. W. Kleij and C. Bo, *Chem.-Eur. J.*, 2013, **19**, 6289-6298.
14. C. J. Whiteoak, A. H. Henseler, C. Ayats, A. W. Kleij and M. A. Pericàs, *Green Chem.*, 2014, **16**, 1552-1559.
15. Q. Liu, L. Wu, R. Jackstell and M. Beller, *Nat. Commun.*, 2015, DOI: 10.1038/ncomms6933.
16. A. T. Najafabadi, *Renew. Sustain. Energy Rev.*, 2015, **41**, 1515-1545.
17. S. Garai, E. T. K. Haupt, H. Bögge, A. Merca and A. Müller, *Angew. Chem. Int. Ed. Engl.*, 2012, **51**, 10528-10531.
18. A. Müller and P. Gouzerh, *Chem. Soc. Rev.*, 2012, **41**, 7431-7463.
19. T. Mitra, P. Miró, A.-R. Tomsa, A. Merca, H. Bögge, J. B. Ávalos, J. M. Poblet, C. Bo and A. Müller, *Chem. Eur. J.*, 2009, **15**, 1844-1852.
20. C. Schäffer, A. M. Todea, H. Bögge, O. A. Petina, D. Rehder, E. T. K. Haupt and A. Müller, *Chem. Eur. J.*, 2011, **17**, 9634-9639.
21. A. Müller, E. Krickemeyer, H. Bögge, M. Schmidtmann and F. Peters, *Angew. Chem. Int. Ed. Engl.*, 1998, **37**, 3360-3363.
22. S. Kopilevich, A. Gil, M. Garcia-Ratés, J. Bonet-Ávalos, C. Bo, A. Müller and I. A. Weinstock, *J. Am. Chem. Soc.*, 2012, **134**, 13082-13088.
23. C. Besson, S. Schmitz, K. M. Capella, S. Kopilevich, I. A. Weinstock and P. Kögerler, *Dalton Trans.*, 2012, **41**, 9852-9854.
24. C. S. Tautermann, A. F. Voegele, T. Loerting, I. Kohl, A. Hallbrucker, E. Mayer and K. R. Liedl, *Chem. Eur. J.*, 2002, **8**, 66-73.
25. M. T. Nguyen, M. H. Matus, V. E. Jackson, V. T. Ngan, J. R. Rustad and D. A. Dixon, *J. Phys. Chem. A*, 2008, **112**, 10386-10398.
26. S. Yamabe and N. Kawagishi, *Theor. Chem. Acc.*, 2011, **130**, 909-918.
27. M. J. Welch, J. F. Lifton and J. A. Seck, *J. Phys. Chem.*, 1969, **73**, 3351-3356.
28. G. A. Gallet, F. Pietrucci and W. Andreoni, *J. Chem. Theory Comput.*, 2012, **8**, 4029-4039.
29. I. Mayer, *Int. J. Quantum Chem.*, 1986, **29**, 73-84.
30. C. Schäffer, A. Merca, H. Bögge, A. M. Todea, M. L. Kistler, T. Liu, R. Thouvenot, P. Gouzerh and A. Müller, *Angew. Chem. Int. Ed. Engl.*, 2009, **48**, 149-153.
31. E. J. Baerends, J. Autschbach, A. Bérces, C. Bo, P. M. Boerrigter, L. Cavallo, D. P. Chong, L. Deng, R. M. Dickson, D. E. Ellis, M. van Faassen, L. Fan, T. H. Fischer, C. F. Guerra, S. J. A. van Gisbergen, J. A. Groeneveld, O. V. Gritsenko, M. Grüning, F. E. Harris, P. v. d. Hoek, H. Jacobsen, L. Jensen, G. van Kessel, F. Kootstra, E. van Lenthe, D. A. McCormack, A. Michalak, V. P. Osinga, S. Patchkovskii, P. H. T. Philipsen, D. Post, C. C. Pye, W. Ravenek, P. Ros, P. R. T. Schipper, G. Schreckenbach, J. G. Snijders, M. Sola, M. Swart, D. Swerhone, G. te Velde, P. Vernooijs, L. Versluis, O. Visser, F. Wang, E. van Wezenbeek, G. Wiesenekker, S. K. Wolff, T. K. Woo, A. L. Yakovlev and T. Ziegler, http://www.scm.com, *Scientific Computing and Modelling* ADF-2012.01.
32. J. P. Perdew, K. Burke and M. Ernzerhof, *Phys. Rev. Lett.*, 1996, **77**, 3865-3868.
33. I. Hyla-Kryspin, G. Haufe and S. Grimme, *Chem. Eur. J.*, 2004, **10**, 3411-3422.
34. E. van Lenthe, E. J. Baerends and J. G. Snijders, *J. Chem. Phys.*, 1993, **99**, 4597-4610.
35. E. van Lenthe, A. E. Ehlers and E. J. Baerends, *J. Chem. Phys.*, 1999, **110**, 8943-8953.
36. E. Van Lenthe and E. J. Baerends, *J. Comput. Chem.*, 2003, **24**, 1142-1156.
37. L. Versluis and T. Ziegler, *J. Chem. Phys.*, 1988, **88**, 322-328.
38. A. Klamt and G. Schüürmann, *J. Chem. Soc., Perkin Trans. 2*, 1993, 799-805.